Cancer Immunol Immunother (2008) 57:1757–1769
DOI 10.1007/s00262-008-0502-9

ORIGINAL ARTICLE

Virulizin® induces production of IL-17E to enhance antitumor activity by recruitment of eosinophils into tumors

Tania Benatar · Ming Y. Cao · Yoon Lee · Hui Li · Ningping Feng · Xiaoping Gu · Vivian Lee · Hongnan Jin · Ming Wang · Sandy Der · Jeff Lightfoot · Jim A. Wright · Aiping H. Young

Received: 16 October 2007 / Accepted: 3 March 2008 / Published online: 20 March 2008

Abstract Virulizin® has demonstrated strong antitumor efficacy in a variety of human tumor xenograft models including melanoma, pancreatic cancer, breast cancer, ovarian cancer and prostate cancer. Our previous studies have demonstrated that macrophages, NK cells, and cytokines are important in the antitumor mechanism of Virulizin®. Virulizin® treatment of tumor bearing mice results in the expansion as well as increased activity of monocytes/macrophages and production of cytokines IL-12 and TNFα and activation of NK cells. In this study we show that the inflammatory cytokine IL-17E (IL-25) is induced by Virulizin® treatment and is part of its antitumor mechanism. IL-17E is a proinflammatory cytokine, which induces a T_H2 type immune response, associated with eosinophil expansion and infiltration into mucosal tissues. IL-17E was increased in sera of Virulizin®-treated mice bearing human melanoma xenografts, compared to saline-treated controls, as shown by 2D gel electrophoresis and ELISA. Treatment of splenocytes in vitro with Virulizin® resulted in increased IL-17E mRNA expression, which peaked between 24 and 32 h post-stimulation. Both in vitro and in vivo experiments demonstrated that B cells produced IL-17E in response to Virulizin® treatment. Furthermore, Virulizin® treatment in vivo resulted in increased blood eosinophilia and eosinophil infiltration into tumors. Finally, injection of recombinant IL-17E showed antitumor activity towards xenografted tumors, which correlated with increased eosinophilia in blood and tumors. Taken together, these results support another antitumor mechanism mediated by Virulizin®, through induction of IL-17E by B cells, leading to recruitment of eosinophils into tumors, which may function in parallel with macrophages and NK cells in mediating tumor destruction.

Keywords Cancer · Eosinophils · IL-17E · Immunotherapy · Virulizin®

T. Benatar · M. Y. Cao · Y. Lee (✉) · H. Li · N. Feng · X. Gu · V. Lee · H. Jin · M. Wang · J. Lightfoot · J. A. Wright · A. H. Young
Research and Development Department,
Lorus Therapeutics Inc., 2 Meridian Road,
Toronto, ON, Canada M9W 4Z7
e-mail: ylee@lorusthera.com

S. Der
Department of Laboratory Medicine and Pathobiology,
Program in Proteomics and Bioinformatics,
University of Toronto, 1 King's College Circle,
Toronto, ON, Canada M5S 1A8

M. Y. Cao (✉)
BGTD, Health Canada, 100 Eglantine Dr., Room 1452-H,
A/L 0603B2, Tunny's Pasture, Ottawa, ON, Canada K1A 0K9
e-mail: ming_yu_cao@hc-sc.gc.ca

Introduction

Virulizin® is an immunomodulator with anticancer properties prepared from bovine bile [1]. Several preclinical reports have demonstrated that administration of Virulizin® suppressed the growth of a wide variety of human tumor xenografts including melanoma, pancreatic, breast, ovarian and prostate cancers [2–4]. Virulizin® lacks direct cytotoxic activity [3], and studies on the anticancer mechanism of action for Virulizin® have shown an essential role for components of the innate immune system, particularly macrophages and NK cells [5, 6]. In vitro, Virulizin® can induce cytotoxic activity of human blood monocytes, peritoneal macrophages, and alveolar macrophages against human tumor cells [1], and stimulate cytotoxicity of the U937 macrophage cell line against tumor cells [7]. Activation of macrophages by Virulizin® significantly increased

the infiltration of NK cells and macrophages into tumor xenografts in mice, resulting in elevated levels of tumor cell apoptosis [5]. Antitumor activity of Virulizin® was substantially compromised in NK-deficient SCID/beige mice [5] and by depletion of macrophages in tumor-bearing nude mice [6]. Mice treated with Virulizin® showed increased levels of NK cells in spleen and peripheral blood, as well as elevated NK cell cytotoxicity in vitro [5] that was diminished following macrophage depletion in vivo [8].

Cytokines are also important in the antitumor activities of Virulizin®. Activation of NK cells following Virulizin® treatment is due in part to expression of IL-12 by activated macrophages [8]. Virulizin® induces macrophage IL-12 production, which in turn stimulates NK cell-mediated antitumor activity [8]. Virulizin®-treated mice have increased expression of IL-12 in peritoneal macrophages, and neutralization of IL-12 with anti-IL-12 antibodies in mice eliminated splenic NK cell cytotoxicity [8]. More recently, it was shown that Virulizin® activates macrophages to produce TNFα in vitro in a dose-dependent manner, and that increased levels of TNFα mRNA were detected in tumor xenografts in mice following Virulizin® treatment [7]. These studies indicate that Virulizin® stimulates several components of the innate immune system that converge in the tumor microenvironment and cooperate to bring about significant antitumor activity.

In the present study we show that the recently described cytokine IL-17E is involved in the anticancer mechanism of Virulizin®. IL-17E (also referred to as IL-25) belongs to a novel family of proinflammatory cytokines that possess significant homology to IL-17 [9, 10]. Although IL-17E is structurally related to IL-17 (IL-17A), its biological effects differ from those described for other IL-17 family members. One striking difference is that IL-17A and IL-17F induce activation and tissue recruitment of neutrophils, while IL-17E is involved in the induction of T helper 2 (T_H2) cytokines and eosinophil recruitment [11]. The expression of IL-17E in mice results in the expansion of eosinophils through the production of IL-5 from an unidentified non-T-cell population [10, 12, 13], and induces elevated gene expression of IL-4 and IL-13 in multiple tissues, resulting in a T_H2-type immune response that manifests as increased serum immunoglobulin E (IgE) levels and pathological changes in the lungs and digestive tract with eosinophilic infiltrates, increased mucus production, and epithelial cell hyperplasia [10, 12, 13]. We show that Virulizin® treatment of tumor bearing mice induces IL-17E expression from B cells, leading to increased blood eosinophilia and infiltration of activated eosinophils into tumors. We also show for the first time that IL-17E has anticancer activity, in addition to its previously described proinflammatory activities.

Materials and methods

Drugs

Virulizin® contains a mixture of both inorganic and organic compounds in a sterile aqueous solution. The active moieties of Virulizin® (Lorus Therapeutics Inc., Toronto, ON) are obtained from bovine bile by a standardized process including ethanol precipitation, column purification, heat reduction, ether extraction, and tyndallization. The drug contains 5% (w/v) solid material and is comprised of inorganic (95–99% of the dry weight) and organic compounds of molecular weights of <3,000 Da (1–5% of the dry weight). Virulizin® is formulated as a sterile injectable solution and is supplied as a 3 ml solution in glass vials with non-latex rubber closures and aluminum tear off caps.

Antibodies and reagents

Antibodies fluorescein isothiocyanate (FITC)-anti-mouse IgM (eB121-15F9; IgG2a), phycoerythrin (PE) anti-mouse CD86 (GL1; IgG2a) and PE anti-mouse CD80 (16-10A1; hamster IgG) were purchased from eBioscience (San Diego, CA). Anti-mouse IL-17E (207710; IgG2b) and PE-anti-mouse CCR3 (83101; IgG2a) antibodies were from R&D Systems (Birmingham, AL). Anti-beta-actin was purchased from Cell Signaling Technology (Danvers, MA). Recombinant mouse IL-17E was purchased from R&D Biosystems.

Cells and animals

Human melanoma cell line C8161 was a gift from Dr. D. R. Welch (Pennsylvania State University, Hershey, PA). Cells were grown in RPMI 1640 medium (Wisent Inc., St Bruno, QC) with 10% fetal bovine serum, penicillin (100 μ/ml), streptomycin (100 mg/ml) (Wisent Inc.) at 37°C under 95% air and 5% CO_2, and maintained with routine media changes. Adherent C8161 cells were passaged by trypsinization with 0.025% trypsin. Single cell suspensions of spleen cells were obtained by meshing and passing through a cell strainer (70 μm; Becton Dickinson, Franklin Lakes, NJ, USA) to separate fibrous tissue. Erythrocytes were lysed with ACK solution (0.155 M ammonium chloride, 0.1 mM disodium EDTA, 0.01 M potassium bicarbonate, pH 7.3) for 5 min on ice. CD-1 athymic nude mice and C57BL/6 mice (6–8 weeks old, 20–25 g, female) were purchased from Charles River (Montreal, QC). The mice were maintained in the animal facility at Lorus Therapeutics Inc. Animal protocols were in compliance with the Guide for the Care and Use of Laboratory Animals in Canada.

Evaluation of anti-tumor activity in a murine model of human tumor xenograft

Human tumor xenografts were established in mice as described [2]. Briefly, human tumor cells were harvested at approximately 80% confluence in cell culture medium and resuspended in sterile PBS. Ten million tumor cells in 100 µl were subcutaneously implanted into the right flank of CD-1 athymic nude mice. When tumors reached a volume of 50–100 mm^3, mice were randomly separated into two groups of ten animals. Mice were treated with intraperitoneal injections of either Virulizin® or PBS (0.2 ml per mouse) daily for 4 weeks. Anti-tumor activity was evaluated as previously described [4]. Tumor volume was estimated by caliper measurements, using the formula: Length × Width × Height/2. Tumor weight was determined from tumor tissue surgically excised from the animal on the last day of the experiment. The percentage of inhibition (%) = (mean tumor weight of control animals-mean tumor weight of drug-treated group)/mean tumor weight of controls × 100. A P value of ≤ 0.05 was considered to be statistically significant.

Two-dimensional gel electrophoresis

Mouse serum was prepared with Aurum Serum Protein Mini Kit (Bio-Rad) to remove albumin and immunoglobulin according to the manufacturer's instructions. The resultant sample was diluted in ReadyPrep Rehydration/Sample Buffer (Bio-Rad) and was subject to 2D gel electrophoresis. First-dimension isoelectric focusing (IEF) was carried out on a Protean IEF cell system as described by the manufacturer (Bio-Rad Laboratories, Hercules, CA). Samples containing up to 20 µg of protein for analytical gels were diluted up to 125 µl with dehydration solution [8 M urea, 2% CHAPS, 50 mM dithiothreitol, 0.2% (w/v) Bio-Lyte 4/7 ampholytes (Bio-Rad) and Bromophenol blue (trace)]. Pre-cast immobilized pH gradient (IPG) strip (7 cm, pH 4–7, linear gradient) (Bio-Rad) was used for the first-dimension separation. Strips were applied by overnight rehydration at 50 V. Then a gradient was applied from 250 to 4,000 V overnight. All IEF steps were carried out at 20°C. After the first-dimension IEF, IPG gel strips were placed in an equilibration solution (6 M urea, 2% SDS, 20% glycerol, 0.375 M Tris–HCl, pH 8.8) containing 2% (w/v) dithiothreitol and shaken for 10 min. The gels were then transferred to the equilibration solution containing 2.5% (w/v) iodoacetamide to alkylate thiols and shaken for a further 10 min before being placed on a 10% polyacrylamide gel slab. Separation in the second dimension was carried out using Tris–glycine buffer containing 10% SDS, at a current of 200 V for 40 min.

For silver staining, gels were immersed in methanol: acetic acid: water (50:5:45) for 20 min followed by washing once in 50% methanol and once with deionized water for 10 min per wash. Gels were pretreated for 1 min in a solution of 2% $Na_2S_2O_3$ and followed by 3 × 1 min washes in deionized water. Proteins were stained with 0.1% silver nitrite for 20 min at 4°C, followed by two washes with deionized water for 1 min per wash. Gels were developed by incubation in 0.04% formalin (35% formaldehyde in water) in 2% sodium carbonate. When the desired intensity was attained, the developer was discarded and reaction stopped by 5% acetic acid. Protein patterns in the gel after silver staining were recorded as digitalized images using a high-resolution scanner. Gel image matching was done with Quantity One software (Bio-Rad).

Peptide mass fingerprinting

Excised gel bands were digested with Trypsin (Promega, Madison, WI) on a ProGest Digestion Robot (Genomic Solutions, Ann Arbor, MI) according to the protocol described [16]. After lyophilization, tryptic peptides were analyzed by liquid chromatography–mass spectrometry (LC–MS) using an Ultimate HPLC system with FAMOS Autosampler (LC Packings-Dionex, Sunnyvale, CA) and LCQ-DECA Ion Trap Mass Spectrometer (Thermo Finnigan, San Jose, CA). Peptides were separated on 75 µm i.d. × 25 cm PicoTip columns packed with 3 µm C-18 beads. The column effluent was sprayed directly into the interface of the Mass Spectrometer. The gradient used for separation was 3–60% of acetonitrile over 25 min. Raw mass spectrometric data were screened against NCBI Data Base using the Mascot Search Engine (Matrix Science, London, UK).

ELISA

ELISAs were performed by coating immunoassay plates (Greiner Bio-One, Longwood, FL) with goat anti-mouse IL-17E Ab (R&D systems) overnight at 4°C. Plates were washed twice with 30× wash buffer (Endogen MiniKits, Pierce Biotechnology, Rockford, IL) and blocked for 1 h at room temp with enzyme diluent (eBioscience) followed by an additional three washes with wash buffer. Serially diluted mouse serum samples were added to the plates and incubated for 2 h at room temp. Plates were washed five times with wash buffer and a 1:200 dilution of rat anti-mouse IL-17E (R&D systems) was added for 1 h at room temp. Plates were washed again five times with wash buffer followed by the addition of a 1:500 dilution of goat anti-rat IgG conjugated to horseradish peroxidase (Amersham Bioscience) for 1 h at room temp. Following an additional eight washes in wash buffer, plates were incubated with

100 µl of 1× TMB substrate (eBioscience) for approximately 15 min in the dark. Finally, 50 µl of Stop solution consisting of 2 N sulfuric acid was added to wells, and absorbance was read at 450/570 nm.

Western blot analysis

Serum samples were prepared as described above. Protein concentration in the lysates was quantified with a Bio-Rad protein assay kit using bovine serum albumin as the standard. Western blotting was performed as described [14]. Briefly, total protein lysates (40 µg/lane) were resolved on 10% SDS-polyacrylamide gels and protein transferred to polyvinylidene difluoride membranes. Blots were treated with blocking agent, 5% nonfat milk in Tris-buffered saline, for 1 h at room temperature. Protein expression was subsequently detected with primary antibodies (described above) at dilutions described in the text. After washing with Tris-buffered saline/Tween 20 three times a secondary antibody conjugated to horseradish peroxidase (Santa Cruz Biotechnology and Amersham Biosciences Inc., Piscataway, NJ) at a dilution of 1:10,000 was added and incubated at room temperature for 1 h. The blots were washed and the immune complexes detected using an enhanced chemiluminescence detection reagent kit (Amersham Biosciences Inc.) and exposed to Kodak X-OMAT AR film for autoradiography.

In vitro stimulation

Spleen cells were isolated from C57BL/6 mice as described above (see "Cells and animals"). Approximately 2×10^7 cells/well were plated in triplicate in six well tissue culture plates after red blood cell lysis. The cells were treated with or without 5% Virulizin® for various time points as indicated. At each time point, adherent and nonadherent cells were harvested and pooled for further analysis.

Reverse transcription-polymerase chain reaction (RT-PCR)

For RT-PCR, RNA was isolated using TRIZOL (Invitrogen, Burlington, ON). Total RNA (2–4 µg) was treated with DNase I to remove any contaminating genomic DNA, and then reverse transcribed into cDNA using 200 units of Superscript II reverse transcriptase (Invitrogen) in the presence of oligonucleotides $(dT)_{12-18}$ according to manufacturer's instructions. Amplification of each target cDNA was performed with JumpStart™ Taq PCR kits (Sigma-Aldrich, St. Louis, MO) in the ABI PRISM 7900HT sequence detection system according to the protocols provided by the manufacturer (Applied Biosystems, Foster City, CA). PCR products were quantified fluorometrically using SYBR Green (BioRad, Mississauga, ON). Two different primer sets were designed and synthesized using Primer Express version 2.0 (Applied Biosystems) for each of the following mouse genes: Interleukin 17E (IL-17E); major basic protein (MBP); eosinophil peroxidase (EPO); interleukin 5 (IL-5); eotaxin-1; β-actin (used as an endogenous control to normalize expression levels among samples). A standard curve of each primer set was generated using mouse genomic DNA. One primer set was chosen for each gene to perform all the subsequent PCR to ensure better PCR efficiency and standard curve lineage.

B cell and T cell isolation

The isolation of splenic B and T cells was performed using EasySep CD19 positive selection protocol for B cells, and EasySep CD90.2 positive selection protocol for T cells (StemCell Technologies, BC) according to manufacturer's instructions. The procedures yielded ≥96% purity.

Flow cytometric analysis

For cell surface marker staining, 1 × 106 cells/sample were incubated with antigen specific antibodies in 100 µl of staining solution (PBS containing 2% fetal calf serum) on ice for 30 min. The cells were subsequently washed twice with staining solution and fixed with 0.5% paraformaldehyde in PBS. Intracellular cytokine staining was performed according to manufacturer's instructions (eBioscience). Briefly, following the final wash cells were fixed by adding 100 µl of Fixation solution for 20 min in the dark at room temperature. Cells were washed once in permeabilization buffer and subsequently resuspended in permeabilization buffer for 5 min prior to addition of anti-cytokine antibody. Anti-IL-17E antibodies were conjugated to biotin, and added to cells at a concentration of 1/20. After a 20 min incubation in the dark at room temperature, cells were washed once and resuspended again in permeabilization buffer, followed by incubation with the secondary reagent, phycoerythrin-Cy5.5-conjugated streptavidin (eBioscience) for 20 min as previously described. Cells were washed once more in permeabilization buffer, resuspended in 0.5 ml of staining solution and stored at 4°C for analysis. Samples were analyzed by flow cytometry using CellQuest software (FACSCalibur, Becton Dickinson, San Jose, CA).

Histochemical detection of eosinophils and computer-assisted image analysis

The excised tumors were fixed in PLP fixative (2% paraformaldehyde containing 0.075 M lysine and 0.01 M sodium periodate solution) overnight at 4°C. The samples were then dehydrated in graded alcohols, embedded in low melting point paraffin and 5 µm sections were cut on a rotary

microtome. Paraffin sections were stained for eosinophils using Sirius red as described previously [15]. Briefly, the sections were deparaffinized, stained with hematoxylin for 2 s, differentiated in distilled water and treated with 70% ethanol for 2 s, then stained with 0.5% Sirius red (Sigma-Aldrich) solution at room temperature for 1 h. After dehydration with increasing concentration of ethanol, the sections were mounted with permount (Fisher Scientific, Pittsburgh, PA).

In vivo injection of recombinant IL-17E

Human tumor xenografts were established as described in CD1-nude mice. Five days posttumor implantation, mice were injected intraperitoneally (ip) with either PBS or Virulizin® daily for 4 weeks, or recombinant mouse IL-17E (1 μg/mouse) (R&D systems) daily for the first 10 days, or recombinant mouse IL-17E (1 μg/mouse) together with Virulizin® daily for the first 10 days, followed by Virulizin® alone for the remainder of the experiment. Mice were sacrificed at four weeks following the start of treatments, and tumors were evaluated as described previously. Peripheral blood was also evaluated for eosinophils by flow cytometry.

Results

Identification of IL-17E in serum of Virulizin®-treated mice

Previous studies demonstrated that Virulizin® has strong antitumor efficacy in a variety of human tumor xenograft models [2–4], and that innate immunity including macrophages and NK cells plays a critical role in the antitumor activity [5, 6, 8]. To further understand the antitumor mechanism of Virulizin®, we used proteomics approaches to investigate the changes of protein expression in serum. Mice with human melanoma C8161 xenografts were treated intraperitoneally with Virulizin® or PBS for 4 weeks. Consistent with previous results [2], Virulizin® significantly inhibited tumor growth as compared to the PBS group (data not shown). The sera were collected from the mice and analyzed by 2D gel electrophoresis. Figure 1a and b show the silver-stained 2D electrophoresis maps of

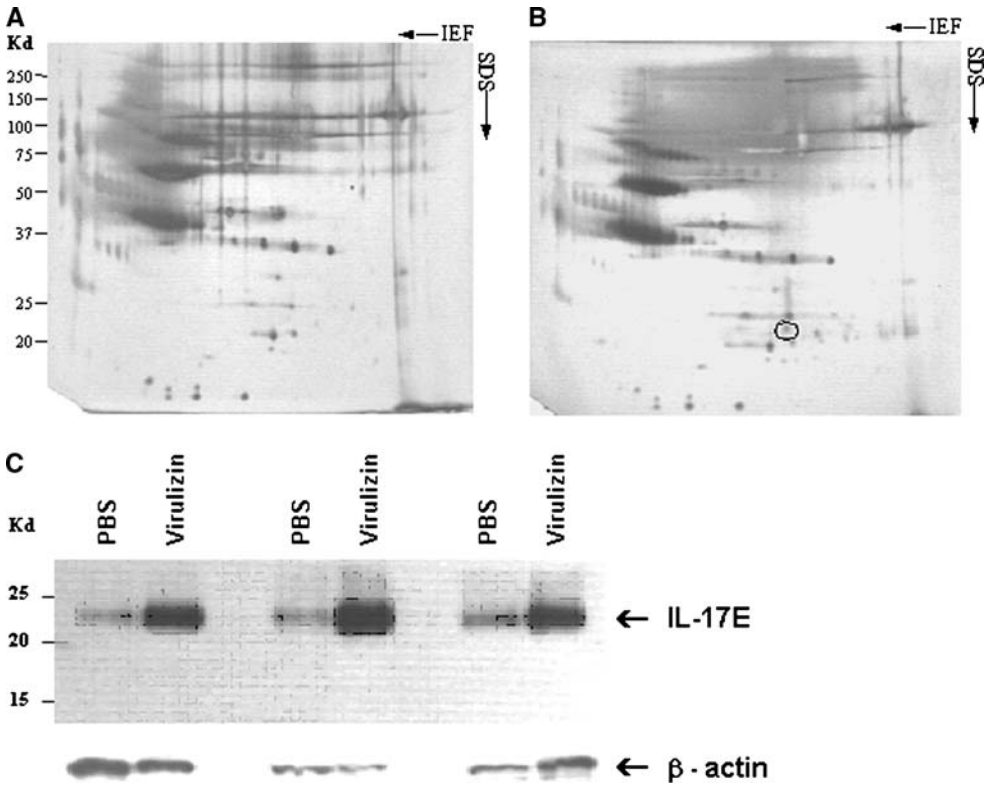

Fig. 1 Identification of IL-17E in mouse serum following treatment with Virulizin®. Human melanoma C8161 cells were subcutaneously injected into the right flank of CD-1 nude mice. The mice were then injected intraperitoneally with 0.2 ml of PBS or Virulizin® daily for 4 weeks. Serum was then collected and analyzed by 2D gel electrophoresis and silver staining. Stained 2D gels are shown from mice treated with (**a**) PBS and (**b**) Virulizin®. One spot (*circle* in **b**) that had higher expression in Virulizin®-treated versus PBS-treated mice was excised and sequenced. **c** SDS-PAGE and Western blot analysis of serum from treated mice. The serum samples were run onto SDS-PAGE gels and proteins were immunoblotted with antibodies against IL-17E (**c**). Western blots of sera from three mice selected at random from each group (Virulizin® or PBS) are shown. Blots were probed with antibodies to *β*-actin to standardize levels of serum protein among wells

sera from PBS- or Virulizin®-treated mice. The intensity of one particular spot (circled in Fig. 1b) was distinctly increased in the serum of Virulizin®-treated mice as compared to PBS-treated mice. This spot was subsequently excised from the gel and analyzed by LC/MS/MS after in-gel digestion. The protein was identified as mouse IL-17E.

Increased level of IL-17E in serum of mice treated with Virulizin®

Serum samples from treated mice were probed in Western blots with anti-mouse IL-17E antibody. As shown in Fig. 1c, a substantial increase in a band with a molecular weight of approximately 23 kDa, corresponding to monomeric IL-17E, was identified in sera of mice treated with Virulizin® as compared to sera of mice treated with PBS. The level of beta-actin on each lane was comparable, indicating equivalent amounts of sera were loaded on the gels. Notably, the size of IL-17E on the Western blot is very similar to the spot detected on silver-stained 2D gel.

To confirm the increased expression of IL-17E in mice following Virulizin® treatment, the sera were collected from mice in antitumor efficacy studies of Virulizin® and analyzed for IL-17E protein by ELISA. As shown in Fig. 2, IL-17E was significantly increased in the sera of Virulizin®-treated mice as compared to those in the PBS controls ($P < 0.001$). The level of IL-17E was elevated from 3.07 pg/μl in PBS-treated mice to 7.73 pg/μl in Virulizin®-treated mice. The results indicate that Virulizin® has a capability of increasing IL-17E expression in mice bearing tumor xenografts.

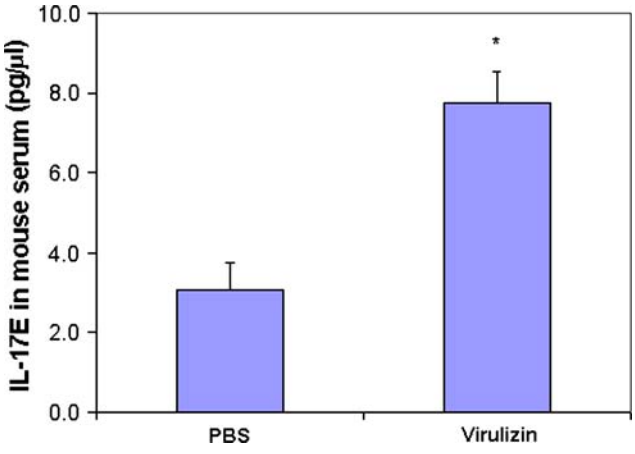

Fig. 2 Increased serum IL-17E in mice treated with Virulizin®. Nude mice bearing human melanoma C8161 xenografts were injected with 0.2 ml of PBS ($n = 8$) or Virulizin® ($n = 9$) daily for 4 weeks. At the end of the experiment serum was collected from mice. IL-17E levels in the sera were determined using ELISA as described in the text. The data represent 3 independent experiments. The detection limit for mouse IL-17E in this assay was <2 pg/μl. *$P < 0.05$ compared to PBS control

Virulizin® induces IL-17E from spleen cells in vitro

To examine whether Virulizin® was capable of directly inducing IL-17E in vitro, splenocytes from naïve C57BL/6 mice were treated with Virulizin® for various time periods and expression of IL-17E mRNA was examined by real-time PCR. As shown in Fig. 3, Virulizin® indeed induced IL-17E mRNA expression from splenocytes, which peaked between 24 and 32 h post-stimulation, with 1.74- and 1.72-fold increase as compare to PBS-treated group, respectively. There was a significant difference in the production of IL-17E from splenocytes derived from Virulizin®-treated mice versus PBS-treated mice, with p values of 0.02 and 0.01 at 24 and 32 h post-stimulation, respectively. A delay in the induction of IL-17E mRNA expression was observed (Fig. 3), suggesting an indirect effect of Virulizin® in the induction of IL-17E. In vitro dose-response studies with increasing concentrations of Virulizin® (1, 5, 10, and 25%) showed that IL-17E was induced in splenocytes at each concentration of Virulizin® tested, with highest levels of IL-17E induced at 25% Virulizin®. However, a clear dose-response relationship was not seen at these concentrations (data not shown).

B cells produce IL-17E predominantly in response to Virulizin®

Splenocytes isolated from C57BL/6 mice are composed of various immune cell populations including B cells, T cells, macrophages and NK cells. In order to determine which cell type was predominantly producing IL-17E in splenocytes

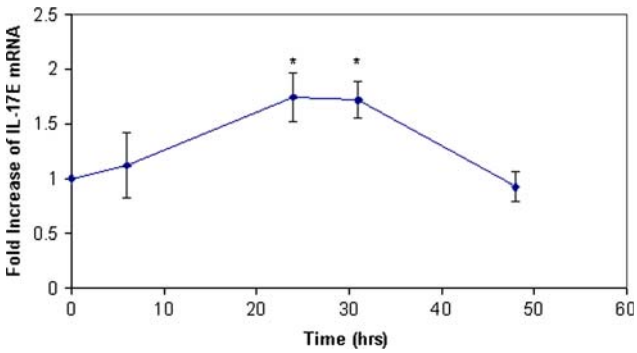

Fig. 3 Quantitation of IL-17E mRNA in splenocytes following treatment with Virulizin® in vitro. Splenocytes were isolated from C57BL/6 mice, and plated in triplicate in 6 well tissue culture plates after red blood cell lysis. The cells were treated with or without 5% Virulizin® for various time points. At each time point, adherent and nonadherent cells were harvested and pooled, RNA was extracted by Trizol method, followed by cDNA preparation. Real time PCR was subsequently performed from the cDNA. Values were normalized to β-actin controls, and then compared to unstimulated samples. Results represent 5–6 experiments per time point. *$P < 0.05$ compared to PBS control

upon Virulizin® stimulation, different cell populations were stained with specific antibodies to surface markers. Flow cytometric analysis of IL-17E expression by intracellular cell staining demonstrated that the responding cell population was IgM+, which established that they were B cells. After treatment with Virulizin® for 72 h in vitro, splenic B cells expressed more IL-17E as compared to unstimulated controls (8.6 vs 2.9%) (Fig. 4a, b). The increase in IL-17E expression by B cells following treatment with Virulizin® in vitro was statistically significant ($P < 0.05$) (Fig. 4c). An increase in IL-17E expression was also observed in the non-IgM + fraction of Virulizin®-treated cells (Fig. 4b) compared to cells treated with PBS (Fig. 4a), indicating that Virulizin® induced IL-17E in other splenic cell populations. This IL-17E+/IgM-negative cell fraction may include T cells, as we found that expression of IL-17E was also slightly induced from splenic T cells after 48 h in vitro treatment with Virulizin® (data not shown). Other cell types, such as macrophages and NK cells in the spleen were sorted by flow cytometric analysis, but IL-17E was not induced from these populations upon exposure to Virulizin® (data not shown).

Virulizin®-induced IL-17E expression in B cells was further confirmed in vivo in CD-1 nude mice, which are congenitally athymic and deficient in T cells [31]. Nude mice bearing C8161 xenograft tumors were treated with Virulizin® for 4 weeks, after which splenocytes were isolated and stained with anti-IgM antibodies followed by intracellular staining for IL-17E. As expected, increased expression of IL-17E was also observed in splenic B cells from CD-1 nude mice (Fig. 5). Flow cytometric analysis showed that the percentage of splenic B cells that expressed IL-17E was significantly higher in Virulizin®-treated mice compared to PBS-treated mice (mean values 13.96 vs 9.20%, $P = 0.04$) (Fig. 5c).

Increased activated splenic B cells in Virulizin®-treated mice

Since IL-17E production was increased in Virulizin®-treated mice and B cells were capable of producing IL-17E, we examined whether Virulizin® affected splenic B cell numbers and activation. Mice with human melanoma xenografts were treated for 4 weeks with either Virulizin® or PBS. The percentage of B cells in splenocytes prepared from treated mice was then determined by flow cytometry using anti-IgM antibodies. We found that B cells were sig-

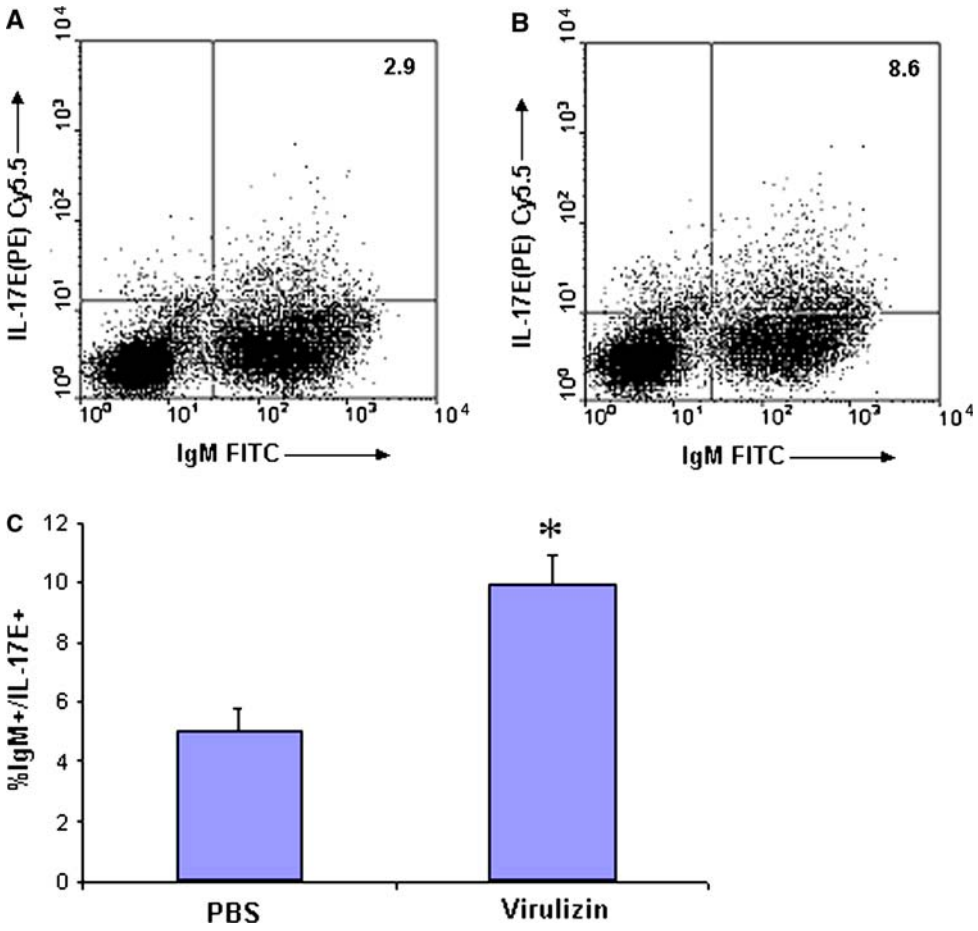

Fig. 4 Virulizin® induces IL-17E expression in splenic B cells in vitro. Splenocytes were isolated and plated in 6 well culture with **a** no stimulation or **b** 5% Virulizin. After 72 h, cells were harvested, surface stained with anti-IgM antibodies, followed by intracellular staining using anti-IL-17E coupled to biotin, followed by phycoerythrin (*PE*)-Cy5.5-conjugated streptavidin. Samples were then analyzed by flow cytometry. Percentages of double positive IgM and IL-17E cells are shown in the *top right quadrant* of each dot plot. The average of 3 separate wells per group was tabulated (**c**). *$P < 0.05$

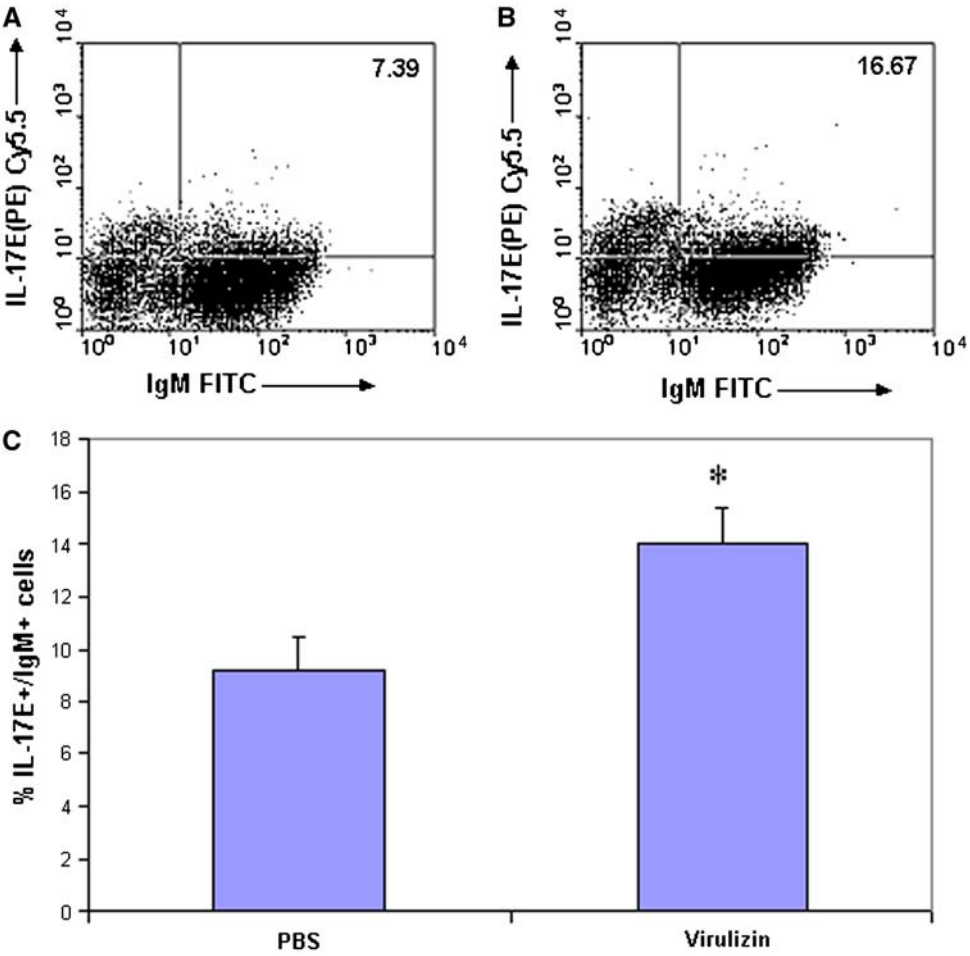

Fig. 5 Virulizin® induces IL-17E expression in splenic B cells in tumor-bearing nude mice. CD1 nude mice bearing human melanoma C8161 xenograft were treated with either PBS or Virulizin® (undiluted) daily for 4 weeks (0.2 ml/day). Splenocytes were isolated and surface stained with anti-IgM followed by intracellular staining for IL-17E. Representative dot plots from flow cytometry analysis of splenocytes from mice treated with PBS (**a**) and Virulizin (**b**) are shown. Percentages of double positive IgM and IL-17E cells are shown in the *top right quadrant* of each plot. The mean percentage of IL-17E positive stained cells from IgM+ gated cells was tabulated (**c**) (*$P = 0.04$; $n = 5$)

nificantly increased in the spleens of Virulizin®-treated mice as compared to controls (72.84 ± 1.9 vs $65.44 \pm 2.1\%$, $P = 0.011$) (Fig. 6a). Furthermore, by double staining with B-cell activation markers CD80 and CD86 we found that there was also an increase in $CD80^+/CD86^+$ B cells in the spleen following Virulizin® treatment as compared to PBS treatment (24.37 ± 2.8 vs $16.31 \pm 1.7\%$, $P = 0.022$) (Fig. 6b). These results suggest that Virulizin® treatment increases the proportion of activated B cells, which may be responsible for the production of IL-17E in Virulizin®-treated mice. Alternatively, IL-17E production may lead to activation of B cells.

Virulizin® induces blood eosinophilia in tumor-bearing mice

Previous work has shown that infusion of mice with IL-17E induced blood eosinophilia and eosinophil infiltration into tissues [10, 13]. Moreover, eosinophil infiltration may lead to tumor regression and can be a prognostic indicator of tumor cell growth [17]. To examine whether Virulizin® could induce blood eosinophilia through induction of IL-17E, eosinophils in the blood of Virulizin®-treated mice were analyzed by flow cytometry using the surface marker for mouse eotaxin receptor, CCR3, which has been shown to be expressed exclusively on murine eosinophils [18]. Mice with C8161 xenografts were treated daily with Virulizin® for 4 weeks, and blood was collected at the end of the treatment period. Flow cytometric analysis showed that blood from Virulizin®-treated mice had higher percentages of CCR3 + cells compared to controls (7.92 vs 3.42%, $P < 0.001$) (Fig. 7), indicating that the number of eosinophils was increased in the blood of Virulizin®-treated mice.

Virulizin® increases eosinophil infiltration into tumors

Blood eosinophilia in Virulizin®-treated mice prompted us to investigate whether there was an increased number of eosinophils infiltrated into tumors, where they may be involved in tumor-killing activities. Mice with C8161 tumors were injected with either PBS or Virulizin® using the treatment schedule described in "Materials and methods". Tumors were excised from mice following a 4-week treatment period, and eosinophil infiltration of tumors was examined by histochemistry studies. Paraffin sections were prepared and stained for eosinophils using Sirius red.

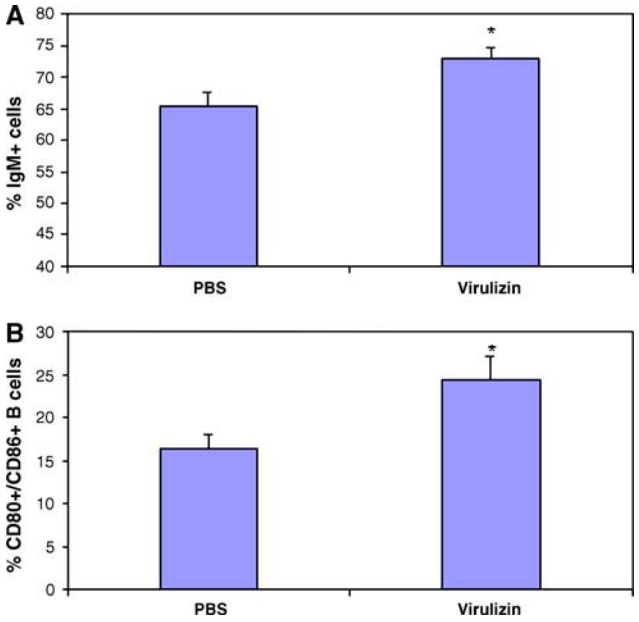

Fig. 6 Virulizin® treatment results in expansion and activation of splenic B cells. Splenocytes from tumor-bearing mice treated daily for 4 weeks with undiluted Virulizin® or PBS (0.2 ml/day) were isolated and surface stained with either **a** anti-IgM FITC for total B cell counts, or **b** anti-IgM FITC + anti-CD80 PE + anti-CD86-PE to measure numbers of activation B cells. As shown in both *panels*, the percentage of B cells (both total and activated) was significantly increased ($P < 0.05$) in Virulizin® treated mice

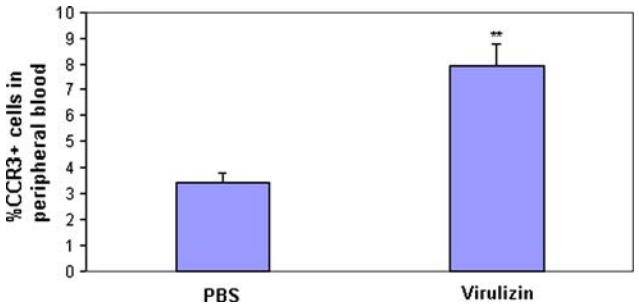

Fig. 7 Virulizin® induces blood eosinophilia. Peripheral blood from tumor-bearing nude mice treated daily with either undiluted Virulizin® or PBS (0.2 ml/day) was collected and red blood cells were removed. The remaining cells were surface stained with anti-CCR3 antibody conjugated with PE and analyzed by flow cytometry. $^{**}P < 0.001$; $n = 31$

Results revealed that there was indeed an increase in eosinophil infiltration into tumors isolated from Virulizin®-treated mice as compared with controls (Fig. 8a). Quantitative image analysis of data obtained from six tumor samples per group demonstrated that the average number of eosinophils per field was approximately 3.5-fold greater in the Virulizin®-treated group as compared to the control group, indicating that eosinophil infiltration was significantly elevated in tumors at 4 weeks following Virulizin® treatment ($P < 0.001$) (Fig. 8b).

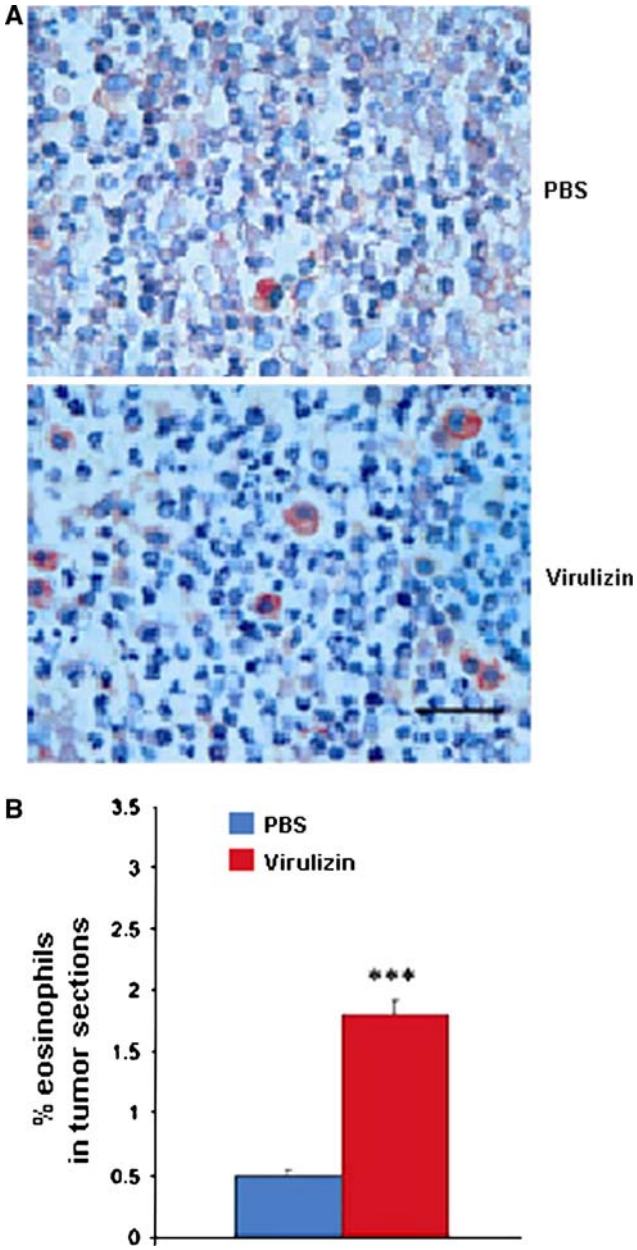

Fig. 8 Virulizin® treatment results in increased recruitment of eosinophils into tumors. CD1 nude mice bearing C8161 xenografts were treated with either PBS or undiluted Virulizin® daily (0.2 ml/day) for 4 weeks. C8161 tumors from treated mice were collected and paraffin sections of tumors were prepared and stained for eosinophils using Sirius Red. **a** Representative micrographs of sections show stained eosinophils in tumors from mice treated with PBS or Virulizin®. A scale bar in each panel represents 25 μm. The number of eosinophils per square millimeter of tumor tissue (**b**) was determined by computer-assisted image analysis. Each bar in the graph represents the mean ± SEM of determinations in six samples of the same treatment. $^{***}P < 0.05$ compared to PBS control

To examine the basis for recruitment of eosinophils into tumors, the expression of cytokine IL-5 and chemokine eotaxin-1 (CCL11) was determined in tumors from Virulizin®-treated mice. Both IL-5 and eotaxin can cooperate to

mobilize and recruit eosinophils from the bone marrow into the tissue through the blood and have been shown to promote infiltration of eosinophils into tumors, correlating with antitumor activity [19–21]. As shown in Fig. 9, both IL-5 and eotaxin were significantly increased in tumors from Virulizin®-treated mice. The results suggest that the recruitment of eosinophils to tumors of Virulizin® treated mice was likely due to IL-5 and eotaxin expression. The identity of the cells that produced IL-5 and eotaxin in response to Virulizin® was not determined.

Increased activated eosinophils in tumors of Virulizin®-treated mice

Eosinophils secrete a number of cytotoxic granule cationic proteins upon activation, including MBP and EPO [22, 23], both of which induce tissue injury and contribute to antitumor cytotoxicity of eosinophils [24, 25]. Eosinophil infiltration in tumors of Virulizin-treated mice was analyzed by real-time RT-PCR for MBP and EPO. Results showed that both markers were increased in tumors isolated from Virulizin®-treated mice compared to PBS controls (Fig. 10), demonstrating that eosinophils found in tumor sites were in fact in an activated state. Taken together, these results suggested that Virulizin® induced the recruitment of eosinophils into tumors, where they became activated, potentially aiding in tumor destruction.

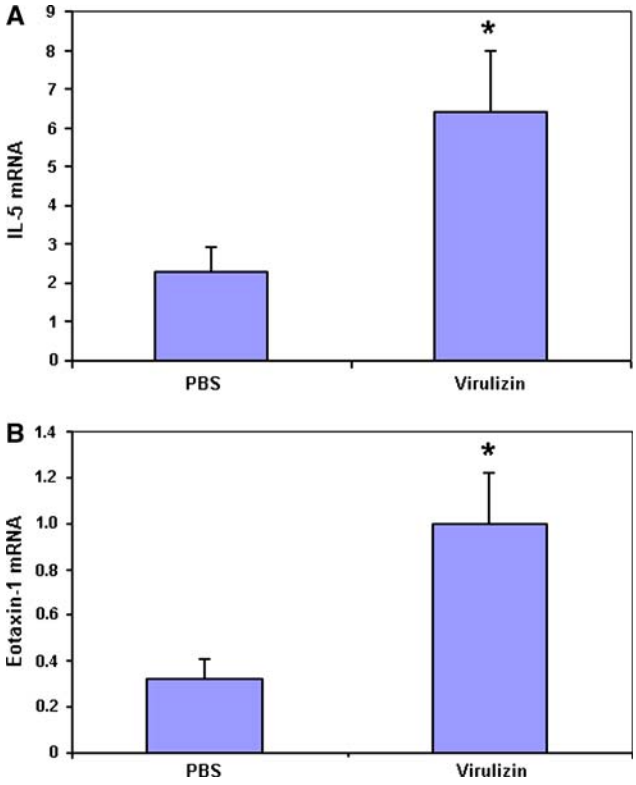

Fig. 9 Quantitation of cytokines IL-5 and eotaxin-1 in human tumor xenografts in mice. Nude mice bearing C8161 melanoma xenografts were treated daily with either undiluted Virulizin® or PBS (0.2 ml/day) for 4 weeks. C8161 xenograft tumors from treated mice were excised and total RNA was prepared from tumor tissues, followed by preparation of cDNAs and quantitative PCR to measure levels of cytokine mRNAs. Levels of IL-5 mRNA (**a**) and eotaxin-1 mRNA (**b**) in tumor tissues were both significantly higher in tumors from mice treated with Virulizin®. Mean values are shown, normalized to levels of β-actin. *$P < 0.05$ compared to PBS control

IL-17E treatment has antitumor activity in vivo

To further confirm that the production of IL-17E was involved in the antitumor mechanism of Virulizin®, xenografted mice were treated with intraperitoneal injections of murine IL-17E to assess antitumor efficacy. Tumor weight measurements revealed that IL-17E treatment elicited antitumor activity, which was comparable to that produced by Virulizin® alone (Fig. 11). Antitumor activity was further enhanced when IL-17E treatment was combined with Virulizin®, although efficacy was not significant when compared to either Virulizin® or IL-17E alone (Fig. 11).

Discussion

This study demonstrates that Virulizin® treatment of tumor-bearing mice results in IL-17E induction and eosinophil expansion in blood and recruitment of activated eosinophils into the tumor microenvironment. Furthermore, we have shown that IL-17E has antitumor activity, which is a previously unrecognized function for this cytokine. The involvement of IL-17E in the antitumor mechanism of Virulizin® adds to our previous studies showing that Virulizin® activates macrophages and NK cells and stimulates the production of cytokines IL-12 and TNF-α [5–8]. A number of other substances have been shown to induce expression of IL-17E (IL-25). Calcium ionophore A23187 in combination with phorbol myristate acetate (PMA) induced IL-25 production in mouse bone marrow-derived mast cells in vitro [26]. In addition, titanium dioxide (TiO2) particles induced IL-25 production when given to rats by intratracheal administration, or when loaded into isolated alveolar macrophages [27]. In these studies, induction of IL-17E was associated with modulation of an inflammatory response. To our knowledge, the current study is the first report of induction of IL-17E by an immunotherapy leading to an anticancer response.

IL-17E has previously been shown to induce blood eosinophilia, eosinophil expansion in spleen and bone marrow, and eosinophil recruitment into tissues [12, 13, 28]. This has been shown following intraperitoneal treatment of mice with recombinant IL-17E (IL-25) [13] and in transgenic mouse models that overexpress either mouse or

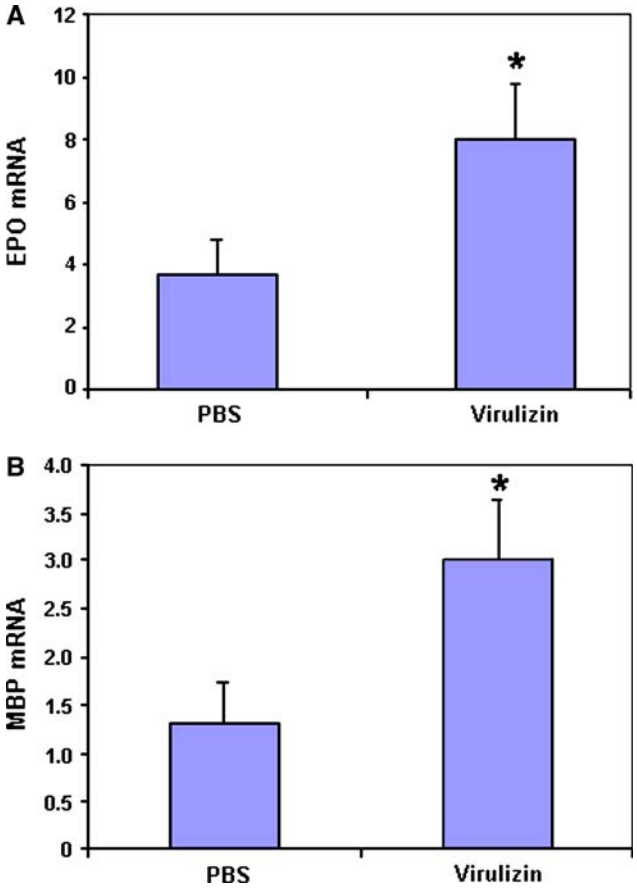

Fig. 10 Quantitation of cytotoxic eosinophil granule proteins in human tumor xenografts in mice following treatment with Virulizin®. C8161 tumor xenografts were excised from mice treated daily with either undiluted Virulizin® or PBS (0.2 ml/day) for 4 weeks, and total RNA was prepared and used for cDNA preparation. Real-time PCR was performed to quantitate eosinophil peroxidase (*EPO*) (**a**) EPO or major basic protein (*MBP*) (**b**). Levels of both EPO and MBP were increased in tumors from Virulizin® treated mice. Mean values are shown, normalized to levels of β-actin. $^*P < 0.05$ compared to PBS control

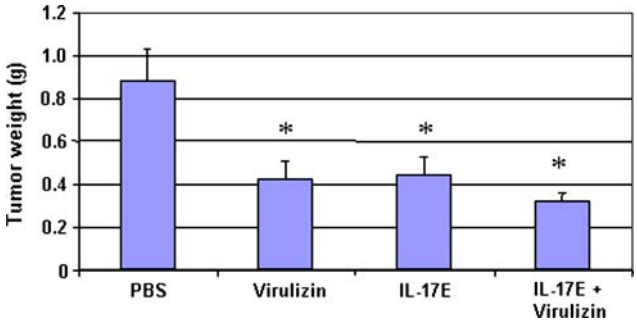

Fig. 11 IL-17E has anticancer activity in vivo. CD-1 nude mice bearing human melanoma C8161 xenografts were treated for 4 weeks with either PBS or Virulizin® daily (0.2 ml/day), or 10 days with recombinant mouse IL-17E (1 μg/mouse), or recombinant mouse IL-17E plus Virulizin® for the first 10 days followed by Virulizin® daily for the remainder of the treatment period (4 weeks). Tumor weights were measured at the endpoint of the experiment. Weights of tumors from mice treated with Virulizin, IL-17E, or a combination of both were significantly reduced compared to those from PBS-treated mice [*P* values: 0.02, 0.02 and 0.004 for Virulizin®, IL-17E, and IL-17E plus Virulizin®, respectively. ($n = 9$)]. Tumor weights from mice treated with both Virulizin® and IL-17E were decreased compared to tumors from mice treated with either agent alone, although this difference was not statistically significant

human IL-17E [12, 28]. In general these studies indicate that eosinophil expansion and infiltration into tissues is part of an overall T_H2-mediated immune response that is associated with organ pathologies, particularly in the lungs and gastrointestinal tract. We did not observe these pathologic changes in mice treated with either Virulizin® or with recombinant IL-17E, indicating that the in vivo levels of IL-17E achieved in our studies are below the threshold required for these toxicities.

Numerous studies have demonstrated a role for eosinophils in tumor immunity, and cancer immunotherapy in particular (reviewed in [22]). Eosinophils produce a variety of cytokines that demonstrate antitumor activities through direct tumor cell killing, as well as indirectly through activation of other immune effector cells in the tumor microenvironment. Clearance of lung and visceral metastases of a CTL-resistant melanoma by T_H2 cells was shown to be dependent on the eosinophil chemokine eotaxin, with degranulating eosinophils within the tumors inducing tumor regression [20]. Activated eosinophils have shown anti-cancer activity in vitro [21], and eosinophil granule proteins released upon activation are highly cytotoxic to tumor cells [24]. Furthermore, eosinophil-derived EPO can synergize with macrophage reactive oxygen species to kill tumor cells [29] or catalyze the oxidation of nitrite to generate additional cytotoxic radicals [30]. Despite these findings, the role of the eosinophil as a cancer effector cell remains controversial, due to conflicting or inconclusive results in different animal models. Recently, a role for eosinophils in tumor immune surveillance and antitumor activity was demonstrated using transgenic mouse models [21]. Transgenic mice that overexpressed IL-5 were significantly resistant to methylcholanthrene (MCA)-induced fibrosarcoma. IL-5 transgenic mice showed a decreased incidence of tumors following MCA injection, and MCA-induced tumors had reduced growth rates compared to tumors induced in wildtype mice. Importantly, both observations significantly correlated with increased eosinophil recruitment into tumors. Similarly, the eosinophil-deficient mouse strains *IL-5/CCL11*$^{-/-}$ and Δ*dblGATA* showed a significantly increased incidence of MCA-induced tumors that correlated with eosinophil tumor infiltration [21]. The results of the present study are supportive of these findings and provide further evidence of the antitumor effects of eosinophils.

The production of IL-17E message has been shown to occur from T_H2 polarized T cells in vitro [13]. Our results

demonstrate that primarily splenic B cells produced IL-17E mRNA and protein in response to Virulizin® both in vivo and in vitro. Previous studies showed that CD19+ B cells were increased in spleens of IL-17E transgenic mice [12]. Consistent with these results, we also found that the proportion of B cells in Virulizin®-treated mice were increased in spleens as compared to PBS-treated controls, suggesting that B cells may be involved in the induction of IL-17E leading to the recruitment of eosinophils. The failure of purified B cells to produce IL-17E in vitro in response to Virulizin® (data not shown) suggests that activation of other cell types is required in order for B cells to produce IL-17E upon Virulizin® treatment. This is further supported by the time delay seen in induction of IL-17E mRNA expression in splenocytes in vitro, suggesting that the cooperative activation of different cells by Virulizin® is required for IL-17E induction in B cells.

The antitumor activity observed through administration of recombinant IL-17E in vivo provides direct evidence for the role of IL-17E in the antitumor mechanism of action of Virulizin®. From our previous studies on the anticancer activity of Virulizin® we have derived a positive feedback model where Virulizin® induces macrophages to produce TNFα and IL-12. These cytokines activate NK cells to produce IFNγ, which in turn activates macrophages. Exactly how IL-17E and eosinophils fit within this model is not known. Our results suggest that induction of IL-17E by Virulizin® leads to eosinophil recruitment into tumors, mediated through increased expression of IL-5 and eotaxin by as yet unidentified cells within tumors. Activated eosinophils that have infiltrated into tumors may have both direct tumor-killing activities through release of MBP and EPO. As well, eosinophils may activate macrophages and NK cells that are present in tumors in response to Virulizin® treatment [5, 8]. Further studies are ongoing to determine the involvement of IL-17E and eosinophils in the context of our current understanding of the antitumor mechanisms of this immune modulator.

In summary, we have identified an additional aspect of the antitumor activity of Virulizin®. The induction of IL-17E by B cells implicates the adaptive immune system as a component of immune induction by Virulizin® and adds to our previous findings showing that Virulizin® activates cells of the innate immune response. Although in vivo expression and administration of IL-17E have shown a variety of pathological changes associated with an inflammatory immune response, these changes have not been observed with Virulizin®, or with the doses of IL-17E used in this study. In a subsequent study we have found that IL-17E has anticancer activity against other tumor types in addition to the antitumor response seen in our melanoma model (manuscript in preparation). These observations suggest that there is potential for the use of IL-17E as an anticancer therapeutic. We are currently investigating this possibility.

Acknowledgments We are grateful to Dr. D.R. Welch for providing human melanoma cell line C8161. We also thank Dr. A. Azad and Dr. J. Wrana at Mount Sinai Hospital, Toronto for technical assistance in peptide sequencing.

References

1. Ferdinandi ES, Braun DP, Liu C, Zee BC, Ely G (1999) Virulizin(R)—a review of its antineoplastic activity. Expert Opin Investig Drugs 8:1721–1735
2. Feng N, Jin H, Wang M, Du C, Wright JA, Young AH (2003) Antitumor activity of Virulizin, a novel biological response modifier (BRM) in a panel of human pancreatic cancer and melanoma xenografts. Cancer Chemother Pharmacol 51:247–255
3. Liu C, Ferdinandi ES, Ely G, Joshi SS (2000) Virulizin-2 gamma, a novel immunotherapeutic agent, in treatment of human pancreatic cancer xenografts. Int J Oncol 16:1015–1020
4. Du C, Feng N, Jin H, Wang M, Wright JA, Young AH (2003) Preclinical efficacy of Virulizin in human breast, ovarian and prostate tumor models. Anticancer Drugs 14:289–294
5. Cao MY, Lee Y, Feng N, Li H, Du C, Miao D, Li J, Lee V, Jin H, Wang M, Gu X, Wright JA, Young AH (2005) NK cell activation and tumor infiltration are involved in the antitumor mechanism of Virulizin. Cancer Immunol Immunother 54:229–242
6. Du C, Feng N, Jin H, Lee V, Wang M, Wright JA, Young AH (2003) Macrophages play a critical role in the anti-tumor activity of Virulizin. Int J Oncol 23:1341–1346
7. Li H, Cao MY, Lee Y, Benatar T, Lee V, Feng N, Gu X, Liu P, Jin H, Wang M, Der S, Lightfoot J, Wright JA, Young AH (2007) Virulizin®, a novel immunotherapy agent, stimulates TNF expression in monocytes/macrophages in vitro and in vivo. Int Immunopharmacol 7:1350–1359
8. Li H, Cao MY, Lee Y, Lee V, Feng N, Benatar T, Jin H, Wang M, Der S, Wright JA, Young AH (2005) Virulizin, a novel immunotherapy agent, activates NK cells through induction of IL-12 expression in macrophages. Cancer Immunol Immunother 54:1115–1126
9. Aggarwal S, Gurney AL (2002) IL-17: prototype member of an emerging cytokine family. J Leukoc Biol 71:1–8
10. Hurst SD, Muchamuel T, Gorman DM, Gilbert JM, Clifford T, Kwan S, Menon S, Seymour B, Jackson C, Kung TT, Brieland JK, Zurawski SM, Chapman RW, Zurawski G, Coffman RL (2002) New IL-17 family members promote Th1 or Th2 responses in the lung: in vivo function of the novel cytokine IL-25. J Immunol 169:443–53
11. Kawaguchi M, Adachi M, Oda N, Kokubu F, Huang SK (2004) IL-17 cytokine family. J Allergy Clin Immunol 114:1265–1273
12. Pan G, French D, Mao W, Maruoka M, Risser P, Lee J, Foster J, Aggarwal S, Nicholes K, Guillet S, Schow P, Gurney AL (2001) Forced expression of murine IL-17E induces growth retardation, jaundice, a Th2-biased response, and multiorgan inflammation in mice. J Immunol 167:6559–6567
13. Fort MM, Cheung J, Yen D, Li J, Zurawski SM, Lo S, Menon S, Clifford T, Hunte B, Lesley R, Muchamuel T, Hurst SD, Zurawski G, Leach MW, Gorman DM, Rennick DM (2001) IL-25 induces IL-4, IL-5, and IL-13 and Th2-associated pathologies in vivo. Immunity 15:985–995
14. Cao MY, Lee Y, Feng NP, Al-Qawasmeh RA, Viau S, Gu XP, Lau L, Jin H, Wang M, Vassilakos A, Wright JA, Young AH (2004) NC381, a novel anticancer agent, arrests the cell cycle in G0–G1 and inhibits lung tumor cell growth in vitro and in vivo. J Pharmacol Exp Ther 308:538–546

15. Wehrend A, Hetzel U, Huchzermeyer S, Klein C, Bostedt H (2004) Sirius red is able to selectively stain eosinophil granulocytes in bovine, ovine and equine cervical tissue. Anat Histol Embryol 33:180–182
16. Houthaeve T, Gausepohl H, Mann M, Ashman K (1995) Automation of micro-preparation and enzymatic cleavage of gel electrophoretically separated proteins. FEBS Lett 376:91–94
17. Tepper RI, Coffman RL, Leder P (1992) An eosinophil-dependent mechanism for the antitumor effect of interleukin-4. Science 257:548–551
18. Grimaldi JC, Yu NX, Grunig G, Seymour BW, Cottrez F, Robinson DS, Hosken N, Ferlin WG, Wu X, Soto H, O'Garra A, Howard MC, Coffman RL (1999) Depletion of eosinophils in mice through the use of antibodies specific for C–C chemokine receptor 3 (CCR3). J Leukoc Biol 65:846–853
19. Samoszuk M (1997) Eosinophils and human cancer. Histol Histopathol 12:807–812
20. Mattes J, Hulett M, Xie W, Hogan S, Rothenberg ME, Foster P, Parish C (2003) Immunotherapy of cytotoxic T cell-resistant tumors by T helper 2 cells: an eotaxin and STAT6-dependent process. J Exp Med 197:387–393
21. Simson L, Ellyard JI, Dent LA, Matthaei KI, Rothenberg ME, Foster PS, Smyth MJ, Parish CR (2007) Regulation of carcinogenesis by IL-5 and CCL11: a potential role for eosinophils in tumor immune surveillance. J Immunol 178:4222–4229
22. Lotfi R, Lee JJ, Lotze MT (2007) Eosinophilic granulocytes and damage-associated molecular pattern molecules (DAMPs): role in the inflammatory response within tumors. J Immunother 30:16–28
23. Rothenberg ME, Hogan SP (2006) The eosinophil. Annu Rev Immunol 224:147–174
24. Kubo H, Loegering DA, Adolphson CR, Gleich GJ (1999) Cytotoxic properties of eosinophil granule major basic protein for tumor cells. Int Arch Allergy Immunol 118:426–428
25. Spessotto P, Dri P, Bulla R, Zabucchi G, Patriarca P (1995) Human eosinophil peroxidase enhances tumor necrosis factor and hydrogen peroxide release by human monocyte-derived macrophages. Eur J Immunol 25:1366–1373
26. Ikeda K, Nakajima H, Suzuki K, Kagami S, Hirose K, Suto A, Saito Y, Iwamoto I (2003) Mast cells produce interleukin-25 upon Fc epsilon RI-mediated activation. Blood 101:3594–3596
27. Kang CM, Jang AS, Ahn MH, Shin JA, Kim JH, Choi YS, Rhim TY, Park CS (2005) Interleukin-25 and interleukin-13 production by alveolar macrophages in response to particles. Am J Respir Cell Mol Biol 33:290–296
28. Kim MR, Manoukian R, Yeh R, Silbiger SM, Danilenko DM, Scully S, Sun J, DeRose ML, Stolina M, Chang D, Van GY, Clarkin K, Nguyen HQ, Yu YB, Jing S, Senaldi G, Elliott G, Medlock ES (2002) Transgenic overexpression of human IL-17E results in eosinophilia, B-lymphocyte hyperplasia, and altered antibody production. Blood 100:2330–2340
29. Nathan CF, Klebanoff SJ (1982) Augmentation of spontaneous macrophage-mediated cytolysis by eosinophil peroxidase. J Exp Med 155:1291–1308
30. van der Vliet A, Eiserich JP, Halliwell B, Cross CE (1997) Formation of reactive nitrogen species during peroxidase-catalyzed oxidation of nitrite. A potential additional mechanism of nitric oxide-dependent toxicity. J Biol Chem 272:7617–7625
31. Immunodeficient Models Datasheet, Charles River Laboratories. http://www.criver.com/flex_content_area/documents/rm_rm_d_immunodeficient_models.pdf